Absolute and Relative Positioning of Natural Organic Matter Acid–Base Potentiometric Titration Curves: Implications for the Evaluation of the Density of Charged Reactive Sites

Marawit Tesfa, Jerome F.L. Duval, Remi Marsac, Aline Dia, José-Paulo F Pinheiro

Absolute and relative positioning of natural organic matter acid-base potentiometric titration curves: implications for the evaluation of density of charged reactive sites

Marawit TESFA*[1], Jérôme F.L. DUVAL*[2], Rémi MARSAC[1], Aline DIA[1], Jose-Paulo PINHEIRO[2]

1 Université Rennes, CNRS, Géosciences Rennes – UMR 6118, F-35000 Rennes, France
2 Université de Lorraine, CNRS, LIEC (Laboratoire Interdisciplinaire des Environnements), UMR 7360 Continentaux, 54500 Vandoeuvre-Lès-Nancy, France

*Corresponding authors. Marawit TESFA (marawit.tesfa@univ-rennes1.fr), Jérôme F.L. DUVAL (jerome.duval@univ-lorraine.fr).

Abstract. Potentiometric acid-base titration curves collected on humic (nano)particles as a function of pH and salt concentration reflect the electrostatics of the particles and the amount of chemical charges (Q) they carry. In turn, interpretation of titration data helps quantifying their reactivity towards metals provided that both intrinsic chemical and non-specific electrostatic contributions to proton binding are correctly unraveled. Establishing a titration curve requires several steps, i.e. blank subtraction, relative curve positioning with respect to electrolyte concentration, and absolute curve positioning achieved by estimation of particle charge Q_0 at low pH. Failure in establishing properly each step may lead to misevaluation of nanoparticle charging behavior. Here, we report (i) a simple procedure to measure and position titration curves for humic substances (HS) versus salt concentration, and (ii) an original approach for absolute curve positioning upon exploitation of proton affinity spectra. The latter do not depend on Q_0 and they thus constrain titration data analysis using Soft Poisson Boltzmann-based Titration (SPBT) formalism for nanoparticles in the thick electric double layer regime. We illustrate the benefits of our approach by analyzing titration measurements for a large range of humic nanoparticles and by comparing the outcome with results from literature.

Synopsis. This article provides a simple and accurate approach to determine the acid-base properties and electrostatic features of humic nanoparticles.

Keywords: Humic substances, Proton titration curves, Potentiometry, Soft particle electrostatics, Nanoparticles.

Graphical abstract

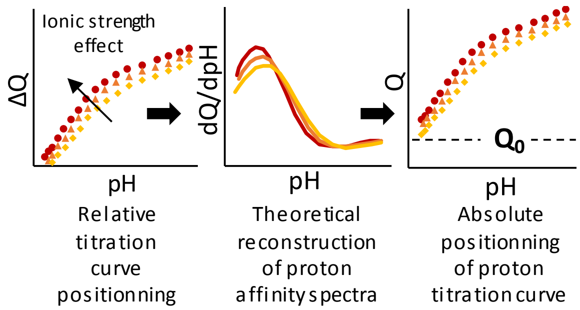

Introduction

Natural Organic Matter (NOM) is ubiquitous in the environment and plays a paramount role in geochemical cycling of elements and in numerous biotic and abiotic chemical reactions.[1–3] NOM has a complex structure, humification state and composition depending on origin, operative hydro-biogeochemical conditions, types and biochemical activity of (micro)organisms that formed NOM by degradation processes. Consequently, NOM reactivity towards a diversity of compounds, including contaminants, remains difficult to understand and predict at a mechanistic level.

Reactions between NOM and protons or metallic contaminants (cations in general) are mainly driven by acid-base functional groups, including carboxylic groups and minor reactive sites such as phenolic groups (amongst sulfur, nitrogen or phosphorous functional groups).[4,5] In this study as in many others related to humic reactivity, only carboxylic and phenolic groups will be considered because they represent the large majority of the proton binding sites. Humic substances (HS) can be divided into humic (HA) and fulvic acids (FA) on the basis of their respective solubility.[6] They are key components of NOM as they carry the majority of carboxylic and phenolic groups. For this reason, the analysis of cation-HS binding processes has been the topic of numerous studies in literature (e.g.[7–13]). Since HS are chemically heterogeneous, a large variety of carboxylic- and phenolic-types of functional groups are found in contrasted chemical environments, and their respective reactivity involves differentiated chemical affinity towards cationic species. In addition, HS are colloids defined by nanometric dimensions, with radii of ca. 1 to 10 nm.[14] They carry an electrical charge resulting from the formation of complexes between cations and reactive sites distributed throughout their intraparticulate volume. The assumption of equilibrium metal complexation by (nano)particulate ligands like HS, as formulated in the commonly adopted Biotic Ligand Model (BLM) and Free Ion Activity Model (FIAM), is tied to the verification of dynamic criteria,[15–17] and for both scenarios of equilibrium and non-equilibrium metal speciation/complexation, the estimation of metal (bioavai)lability in suspension containing (nano)particulate ligands like HS requires proper evaluation of HS metal binding sites, metal binding heterogeneity and a proper integration of the HS electric double layer properties.[18–21] This is where proton titration method comes in as this method allows for the determination of these properties.

Because cations and protons compete for the same binding groups, it is fundamental to determine HS acid-base properties, which includes amounts and dissociation constants of carboxylic and phenolic groups. For that purpose, acid-base potentiometric titration curves are commonly collected as a function of pH and salt concentration, and subsequently analyzed by thermodynamic modeling.[22,23] The method consists in performing successive acid-base titrations for a given HS sample dispersed in a monovalent background electrolyte (e.g. NaCl, KNO_3), whose concentration is generally increased to achieve three ionic strengths (IS) typically in the range 3 to 300 mM. The sample is first acidified to reach the lowest chosen pH value ($3 \leq pH \leq 4$) at the lowest salt concentration adopted for the measurement. Then, the sample is titrated with a base, up to the highest chosen pH (typically $10 \leq pH \leq 11$), followed by an acid titration back to the original pH. These titrations are repeated to obtain replicates at fixed salt concentration (forward and reverse measurements). To increase IS, salt is added at the lowest pH and titration procedure is then iterated for the second and third IS condition tested. The evaluation of the amount of H^+ or OH^- consumed by HS provides a direct quantification of the number of deprotonated groups as a function of pH over the whole HS dispersion volume. This number can then be converted into a variation of the (negative) electrical charge carried by HS (denoted as ΔQ) relative to the charge of the material at the initial pH of the titration curve (denoted hereafter to as Q_0). Analysis of the dependence of HS charge variation on pH and salt concentration further requires adequate estimation of the chemical (intrinsic) and electrostatic (non-specific) contributions to the proton affinity for HS carboxylic and phenolic groups, which requires modeling.[17,19-24]

Despite of the apparent simplicity of the aforementioned proton titration procedure, major experimental challenges must be addressed to achieve accurate determination of HS acid-base properties. Two of them are listed below:

(i) A major difficulty concerns the estimation of the absolute charge (Q) of HS materials as a function of pH. Even though the necessity to assess Q_0 value is recognized to compute Q from ΔQ, there is, to the best of our knowledge, currently no clear method proposed to evaluate Q_0. In literature, the way Q_0 is estimated is either not described[25–27] or tied to its adjustment within multiparametric modeling-based fitting exercise.[28,29] A possible way to estimate Q_0 would consist in measuring the point of zero salt effect (PZSE). However, this option is impossible to set in practice as for most HS materials the PZSE corresponds to pH values much lower than 3, i.e. conditions where HS charge tends to 0 and HS are prone to the formation of aggregates (especially so for the humic fraction).

(ii) The positioning of the different IS curves relatively to one another (hereafter referred to as “relative curve positioning”) requires an additional independent salt titration at a chosen fixed pH, commonly known as pH stat salt titration.[30] This option is not optimal because of the additional measurement time it requires and the possible associated uncertainties in the ensuing relative curve positioning process brought by the analysis of a different sample.

Theoretical evaluation of HS charge properties from acid-base titration data is also highly challenging. Substantial efforts have been made to estimate thermodynamic proton- and metal ion-HS binding parameters and to develop predictive models under environmentally relevant conditions.[4,7,10,25,29,31–34] Historical models on protons binding by HS treat humic substances as mixtures of dissolved aqueous solutes. Most of these models trace their origin to the Langmuir equation. The Henderson-Hasselbalch equation, a linearized logarithmic version of the Langmuir equation, can be represented using multiple Langmuir sites, which leads ultimately to the Gaussian distribution model. The Freundlich model is an entirely empirical isotherm allowing infinite binding in its unbounded original form; this model is nearly equivalent to a Gaussian distribution of Langmuir binding sites in its bounded form, as mathematically proven by Sips.[35] The well-known hybrid Langmuir-Freundlich model (whose linearized logarithmic form is known as the modified Henderson-Hasselbalch equation), often involves two types of sites to describe proton binding on HS and to fit experimental data for complex HS mixtures. Other models like Models WHAM V or VI may integrate more binding sites (up to 8) and they came as improvement to the aforementioned pioneering theoretical representations as they included effects associated to electrostatics of HS viewed as particles and not as solutes. Indeed, previous study[36] demonstrated that HS electrophoretic properties, in particular their dependence on solution ionic strength, could be properly interpreted using electrohydrodynamic theory for soft (ion-permeable) particles. The successful interpretation also applied to large ionic strengths where historical electrokinetic models valid for solutes or molecules (e.g. Hückel-Onsager formalism) failed in reproducing quantitatively the peculiar electrokinetic behavior of soft particles under such electrolyte concentration conditions.[37,38] As a further support for representing HS materials as (nano)particles rather than solutes, we mention that the chemodynamics of metal-humics or metal-fulvics complexes (which refers to the interconversion kinetics between free and complexed metal forms) cannot be understood at a quantitative level on the basis of the well-known Eigen metal complexation model that is strictly applicable to ligands of small molecular size.[39] Instead, a kinetic model elaborated with a nanoparticulate representation of humics with adequate electrostatics evaluated from Poisson-Boltzmann theory for soft nanocolloids was shown to correctly capture the way kinetics of metal association with humics and fulvics depends on particle size and electrostatic properties as well as on the metal nature.[39] The remarkable dynamic reactivity of nanoparticulate humics and fulvics originate from Boltzmann metal accumulation and Debye acceleration of metal transport, most pronounced for soft particles that exploit accelerating mechanism on a 3D level.[39] Last, we emphasize that measured diffusion coefficients of humics and fulvics, in the range 2.5×10^{-10} $m^2\ s^{-1}$ to 6.9×10^{-11} $m^2\ s^{-1}$ for two of the samples analyzed here (i.e. Suwannee River Natural Organic Matter and Pahokee Peat Humic Acid)[40] better fit a particle-based representation for HS rather than a molecular/solute one. Typical diffusion coefficients for molecules range indeed from 6.23×10^{-10} $m^2\ s^{-1}$ (for citric acid ~200 g mol^{-1}) to 4.14×10^{-10} $m^2\ s^{-1}$ (for rhodamine 6G ~500 g mol^{-1}).[41,42]

Further benefits in adopting Poisson Boltzmann theory for HS particles were evidenced by Pinheiro et al.[17] in their analysis of potentiometric titration curves collected for a large variety of HS. In detail, these authors reported a formalism called SPBT-PEST (SPBT for Soft Poisson Boltzmann-based Titration theory and PEST as the module used for adjustment of SPBT-parameters) to reconstruct experimental titration data on proton binding to HS with an analysis based on rigorous numerical solving of non-linearized Poisson-Boltzmann equation for soft nanoparticles. Practically, SPBT-PEST analysis of potentiometric titration data involves the concomitant reconstruction of both the measured titration data and the associated proton affinity spectra over the whole range of pH and salt concentration conditions tested. It is stressed that the SPBT-PEST model, when applied to chemical conditions where there are no electrostatic effects, identifies with the Henderson-Hasselbalch equation. Within adopted particle-based representation of HS, the Langmuir-Freundlich or Henderson-Hasselbalch isotherm may be applicable, albeit at a local level within the reactive body of the HS, and the binding properties perceived at the scale of the particle and that of the particle dispersion must then be retrieved from proper spatial integration, as detailed elsewhere.[17]

Given the aforementioned elements, WHAM model VI/VII involving simple solution to the Poisson-Boltzmann (PB) equation valid for hard particles (i.e. impermeable to ions from background electrolytes), is unsuitable for HS, as further argued by Town et al.[43] and Rotureau et al.[44] in the context of equilibrium metal binding to HS. Whereas NICA-Donnan model represents HS as permeable spheres, the electrostatic potential profile associated to Donnan representation is oversimplified as it implies a potential that is *a priori* constant inside the particle. However, this simplification may result in a misevaluation of the proton and metal ion-HS binding parameters as variation of inner particle potential with position is operational in small-sized particles like many HS for which radius is comparable to Debye length.[19,43,44] Furthermore, the Tipping models or NICA-Donnan model do not allow a quantitative interpretation of metal stability constants and heterogeneity thereof as measured with electroanalytical techniques in media differing with respect to ionic strength.[19,43,44]

As a response to the major limitations and challenges identified above, we develop herein a new experimental and theoretical procedure allowing for a consistent determination of acid-base HS features. We show that the new experimental approach we propose leads to: (i) a reduction of the overall measurement time by a factor ~3, (ii) a decrease of effects related to sample dilution, and (iii) an improved relative positioning of titration data curves collected on a given sample at different electrolyte concentrations. The data treatment process involves the direct subtraction of an experimental blank to measured sample, and a robust method - here explicitly detailed - for the evaluation of the absolute charge Q from the relative charge variation ΔQ measured with changing pH and salt concentration. This evaluation is achieved by exploiting proton affinity spectra defined as the first derivative of the titration curve with respect to pH (dQ/dpH), spectra that do not depend on Q_0. The parameters describing the intrinsic heterogeneity of HS reactive sites as well as the chemical and electrostatic HS components to proton binding mechanism are then recovered by consistent reconstruction of both proton affinity spectra and titration data using SPBT-PEST model.[18] Our approach is illustrated with measurements on several widely used HS standards provided by the International Humic Substance Society (IHSS).[25,26,45,46] To the best of our knowledge, no acid-base titration data has ever been reported for the most recent samples commercialized by the IHSS. The obtained results are compared with ones published on these IHSS samples collected at the same location but ca. 30 years ago.[26]

Materials and Methods

Reagents. All 7 HS samples analyzed in this work were purchased from IHSS, their abbreviated names adopted in this study together with their reference number are indicated in brackets: three samples from Suwannee River, one humic acid, one fulvic acid and one natural organic matter (respectively SRFA, 3S101F; SRHA 3S101H and SRNOM 2R101N), two from Pahokee Peat fulvic and humic acid (respectively PPFA, 2S103F and PPHA, 1S103H), and two humic acid samples from Leonardite (LHA, 1S104H) and from Elliot Soil (ESHA, 4S102H). Reagents needed for the titration were acquired from Sigma Aldrich, namely acid (HCl, 0.1 mol L^{-1}), base (NaOH 0.1 mol L^{-1}) and background NaCl electrolyte. The pH-buffer solutions required for electrode calibrations were ROTI®Calipure products (pH 4.00, 5.00, 7.00, 9.00, 10.00). All samples were prepared with Ultrapure Water provided through a Milli-Q purification system.

Instruments. All pH measurements were performed by a Hamilton Fluxtrode pH electrode. Mettler Toledo analytical balance (±0.0001 g) was used to weigh all HS samples. Acid, base and salt additions during titration and HS dispersion process were conducted with an automated Metrohm titrator 809 Titrando, connected to a TIAMO v2.4 program that operates three burettes. Regarding the burettes, two of them had a volume of 10 mL and one of 2 mL, and they were respectively filled with 0.1 M HCl, 2 M NaCl and 0.1 M NaOH solutions. A TIAMO script was written for the titration protocol and is available on request.

Sample preparation. Sample solutions were prepared by mixing 25 mg of HS material, 50 ml of 1 mM NaOH and 9 mM NaCl directly into the titration Teflon vessel. The resulting sample concentration (i.e. 500 mg of NOM L^{-1}) adopted in this work and in other studies[47–49] is optimal for the detection of variation in HS charge with changing solution pH as it avoids e.g. the addition of large volume of titrants with use of sufficiently high concentrations in acid and base. Christl et al.[50] investigated the effects of humic and fulvic acid concentrations (1-1000 mg/L) and ionic strength on copper and lead binding, and found that corresponding metal-binding isotherms measured at high and low humic matter concentration were similar. Reversible aggregation-disaggregation of HS particles may occur and aggregation issue is more significant for humic acids than for fulvic acids. Particle aggregation is further most important at low pH and high ionic strength. As we change the ionic strength at high pH (see titration protocol in the next section), thereby spending far less time at low pH condition, we expect that this specific aggregation problem will be less severe with the new titration methodology proposed here. Our HS disaggregation protocol is applied to ensure that the dissolution of the solid material is complete and that there is no significant amount of aggregates in solution. We emphasize that the experimental verification (via diffusion coefficient measurement by Dynamic Light Scattering, DLS, or by voltammetry[17]) for the occurrence or not of HS particle aggregation under the conditions used for the titration measurements is not an easy task as e.g. DLS will be affected by multiple scattering at the HS concentration of interest and voltammetric measurements by the absence of signal as all cadmium ions will be then strongly complexed. The vessel was placed in an ultrasonic bath for 1 minute to disperse any possibly occurring aggregates. It was then placed in a thermoregulated glass vessel at 25°C under argon atmosphere, and the solution was magnetically stirred during the entire titration experiment. Subsequently, HS disaggregation protocol was initiated with a Titrando stand: HS solution was first set at pH 10 using NaOH 0.1 M and the pH decrease was monitored during 1 hour. Then the pH was set again to 10 and monitored overnight (usually 12 hours). Afterwards solution pH was set at 3 using HCl 0.1M, just prior to application of the potentiometric titration protocol detailed below.

Potentiometric titration protocol. Each sample titration was paired with a corresponding blank titration performed either before or after sample titration. The hereafter-described protocol applies to both the blank and the sample titration step. Five pH-buffer solutions (pH = 4, 5, 7 and 9 and 10) were used to determine a pH-potential (E, in V) calibration curve for the pH electrode prior and subsequent to a titration process (for both blank and sample measurement). All titrations were conducted between pH 3 and 10.5 using potential control. For each sample and associated blank measurement, titrations were successively conducted at three solution ionic strengths: 10 mM, 30 mM and 100 mM NaCl. One of the main aspects of the new experimental protocol is that the initial (E_{start}) and final (E_{end}) potential values - for all three IS conditions in both blank and sample titrations - are rigorously kept equal to minimize error in blank subtraction and curve positioning procedure.

After ensuring that E is stable for at least 15 mins and that it equals E_{start} (corresponding to pH 3, IS =10 mM), the sample or blank solution was titrated with a base solution, with increasing solution pH up to 10.5 (corresponding to E_{end}). Then, IS was increased from 10 mM to 30 mM upon addition of 2 M NaCl solution. This led to a drift of E to a larger value (E_{drift}), which was carefully monitored until it stabilized (within 15 min). After stabilization, E was set again to E_{end} upon addition of a small volume of 0.1 M NaOH solution. The added amount was recorded and used later for relative curve positioning purpose. Subsequently, acid titration (using 0.1 M HCl) was performed to reach E_{start}. The entire procedure was repeated with: (i) a base titration up to E_{end}, (ii) an increase in IS to 100 mM NaCl concentration, (iii) a careful monitoring of E_{drift}, (iv) an addition of base to reach E_{end} again, and (v) a reverse and forward titration with acid and base, respectively.

We cautiously verified the correct electrode calibrations at the start and end of the titration experiments as these were found identical within experimental error, meaning that we did not observe any calibration drift in the course of the titration experiments.

The deprotonated groups carried by the HS (Q_{HS}) are determined by point-by-point subtraction of the blank titration for each pH condition tested [51,52] (eq 1).

$$Q_{HS} = Q_{HS+solution} - Q_{blank} \qquad (1)$$

where $Q_{HS+solution}$ and Q_{blank} represent the number of mols per liter of added titrant in the presence and absence of HS, respectively. This operation leads to estimation of Q_{HS} solely associated with HS titration with a reference of 0 moles L^{-1} of charge at pH 3 and 10 mM salt concentration as the Q_0 value is unknown at this stage of the analysis. ΔQ (in mol kg^{-1}) was then calculated by dividing the blank-subtracted Q_{HS} value by the concentration of HS ([HS] in kg L^{-1}) (eq 2):

$$\Delta Q = \frac{Q\mathrm{HS}}{[\mathrm{HS}]} \qquad (2)$$

Fitting procedure. The SPBT-PEST fitting procedure applied to obtain the parameters that best describe the experimental titration curves and their associated proton affinity spectra closely follows the one proposed by Pinheiro et al.[18] except for the very determination of Q_0. This procedure is described in detail in section C of the Supporting Information (SI) of the paper by Pinheiro et al.[18] the reader is referred to. The procedure consists in three steps that we briefly recall:

a) Initial parameter estimation

The input file needed to run SPBT-PEST model is a file containing the measured charge vs. pH and its associated proton affinity spectrum (dQ/dpH vs. pH). This affinity spectrum was obtained by cubic spline interpolation of the experimental Q vs. pH curve and evaluation of its derivative with respect to pH (step achieved using Matlab™ software). The required estimation of the particle radius (r_p, in m) and molecular weight (M_w, in kg mol^{-1}) is done along the lines detailed in the sections A and B of SI. Briefly, scanned stripping chronopotentiometry (SSCP) was used to determined r_p [53] and values of M_w or realistic ranges thereof (minimum: $M_{w,min}$ to maximum: $M_{w,max}$) were inferred from literature review. Guessed values for the density of reactive carboxylic and phenolic groups (in mol kg^{-1}) were estimated from the experimental ΔQ vs. pH curve, namely: carboxylic sites density ($Q_{max,1}$) was set equal to the value of ΔQ reached at the first plateau encountered with increasing pH, density of phenolic groups ($Q_{max,2}$) was set equal to the excess of measured charge relative to that plateau value. The initial guessed values for the protonation (or dissociation) constants pertaining to carboxylic and phenolic groups (pKa_1 and pKa_2, respectively) were estimated from direct reading of the pH position of the maxima in the proton affinity spectrum (dQ/dpH vs. pH). The parameters describing the chemical heterogeneity of carboxylic and phenolic groups (m_1 and m_2, respectively) were initially set to 0.5 value according to the procedure described in section D of Pinheiro et al. [18]. All values adopted for the initial guessed estimates of the relevant parameters listed above are collected in Table S1 in SI (section C therein) for the IHSS samples of interest in this work. They serve for initiating the iterative procedure detailed by Pinheiro et al.[18] to recover the measured proton titration data and associated proton affinity spectra.

b) Q_0 determination

The novel determination of Q_0 proposed in this work involves the exploitation of the proton affinity spectrum (dQ/dpH), which can be calculated from the measured pH-dependence of the charge variation (ΔQ) as formulated by eqs. 3 and 4:

$$Q = \Delta Q + Q_0 \tag{3}$$

$$\frac{\mathrm{d}Q}{\mathrm{dpH}} = \frac{\mathrm{d}\Delta Q}{\mathrm{dpH}} \tag{4}$$

Concomitant fitting of the proton affinity spectra, derived from the data measured at the three adopted IS values, provides a full set of estimated parameters (r_p, M_w, $Q_{max,1}$, $Q_{max,2}$, pKa_1, pKa_2, m_1, m_2). These parameters where obtained by adjustment of data with SPBT-PEST formalism, and they are -by construction- independent of any arbitrary choice made for Q_0. These parameters then serve to compute newly corrected Q vs. pH curves for all three IS where the value of Q_0 corresponds to the lowest Q value, i.e. at pH 3 and 10 mM NaCl.

c) Refining the parameter values

Refinement of the parameter values (r_p, M_w, $Q_{max,1}$, $Q_{max,2}$, pKa_1, pKa_2, m_1, m_2) is subsequently made from concomitant SPBT-PEST-based analysis of both Q and dQ/dpH curves following steps 3a and 3b in section C of the SI of Pinheiro et al..[18] The fitting procedure is first applied by setting r_p and M_w to constant values while refining $Q_{max,1}$, $Q_{max,2}$, pKa$_1$, pKa$_2$, m_1, m_2, and then upon refining r_p and M_w whereas setting the other parameters constant.

It is stressed that adopted SPBT-PEST modeling is performed without including any specific binding of Na^+ to HS, that is by regarding the background electrolyte medium as indifferent with no role of the electrolyte ions in the processes that control the pristine structural charge of the HS particles.[17] This approximation, also made within NICA-Donnan based modeling framework,[20] is legitimate due to the extremely weak binding of Na^+ to any ligand in solution, as illustrated by its tendency to poorly hydrolyze (corresponding pK approximately equal to 14).[54]

Results and discussion

This section reports HS titration data measurements and theoretical treatment on the basis of our proposed experimental protocol, namely blank subtraction, relative positioning of the experimental titration curves at different IS and the absolute curve positioning once the charge Q_0 at low pH is determined. Best fitted parameters from SPBT-PEST modeling of the data on studied IHSS batches are given and compared with previously published results.

Blank subtraction. An example of blank, raw and blank-corrected sample titration curve (Q_{exp} vs. pH) is given for Suwannee River Fulvic Acid (SRFA) at 10 mM NaCl in Figure 1. The blank correction is classically conducted by theoretical interpolation of the experimental blank titration curve and subsequent subtraction to sample titration data over the whole range of pH values where they have been collected. Nevertheless, in addition to the exclusion of electrode drift in the blank data fitting operation, the equation used for theoretical interpolation of blank titration data poorly fits pH domains where steeped variations in material charge are measured. These errors introduced during blank correction may, in turn, leads to erroneous "blank corrected" curves of titrated sample. In order to compute a blank correction that integrates electrode drift (if any) and truly represents experimental blank titration curve, the experimental blank values were fitted by cubic spline function using Matlab™ software. This makes possible the blank subtraction from sample titration data to be performed point by point.[51,52] It is emphasized that accurate experimental blank subtraction is possible if and only if blank and sample titration curves start and end exactly at the same electrode potential (E_{start} and E_{end} respectively), so as to minimize errors in pH domains where steep sloped sections are measured, namely at low and high pH values. Last, additional smoothing of the cubic spline function retrieved from blank titration data interpolation may be necessary in case of noisy blank titration data, recalling that specificity of cubic spline function is that it has to pass through all experimental data points subjected to interpolation.

As expected, resulting corrected titration curves obtained for all studied IHSS samples display a negative charge over the whole pH range studied, which is typical for natural organic matter.[55–59]

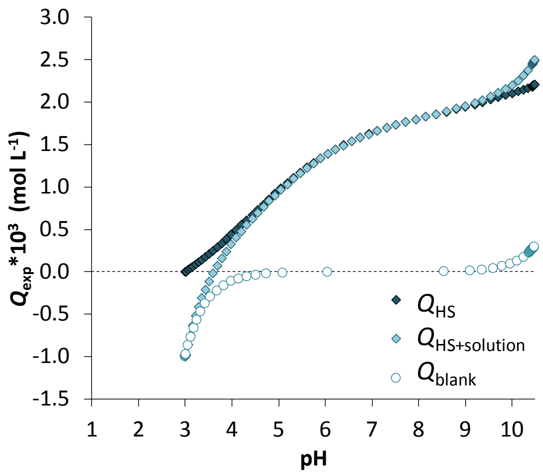

Figure 1: Experimental titration data versus pH. The Q_{HS} is computed from eq 1 determined at 10 mM background electrolyte solution for the blank solution (Q_{Blank}), the paired SRFA-containing solution ($Q_{HS+solution}$) and the difference between these data (Q_{HS}) are represented. The initial charge (pH 3) for the raw ($Q_{HS+solution}$) and blank (Q_{HS}) titration is given by the number of moles of acid anions [Cl-], and subsequent points are computed by adding the number of moles of cations of the titrant [Na+].

Relative positioning of titration curves at different salt concentrations.

Background electrolyte concentration affects proton-HS binding as it impacts the electrostatic contribution to the overall interaction between HS and protons. As a direct consequence, evaluation of this electrostatic component of HS reactivity towards protons critically depends on the relative position of the titration curves measured at different solution ionic strengths. For the sake of illustration, Figure S1 (section D in SI) shows a flawed relative positioning of titration curves for SRFA "FH-03" sample given by Milne et al.[25] Unlike curves well positioned with respect to electrolyte concentration (Figure S1), data (measured at 2, 10 and 100 mM NaCl) by Milne et al.[25] display overlap over the entire range of pH values. As a consequence, the interpretations derived from such titration curves presenting an overlap would imply that the titrated HS material would have the same proton binding behavior regardless of solution ionic strength IS, whereas opposite conclusion was extensively reported in literature.[17] In Figure 2, titration curves of SRFA at three IS were positioned following the new procedure detailed in the preceding section. According to our proposed methodology, salt addition is carried out at the highest pH value when E_{end} is reached at the end of the base titration (step 1). Under such conditions, HS charge and corresponding attractive electrostatic HS-H^+ interactions are maximal.[60] This leads to a significant release of H^+ into the solution, which can be (i) accurately monitored through pH-electrode (E = E_{drift}) as the charge variation exceeds electrode-measurement error, and (ii) neutralized by precise addition of OH^- to reach E_{end} again (step 2). The same procedure is carried out in the blank titration were the amount of OH^- necessary to return to E_{end} is due to dilution effect. The difference of base number of moles, needed to return to E_{end}, between sample and blank titration, represents the new HS charge resulting from increase in salt concentration. To position the titration curves, the result of the equation 2 is summed to the new HS charge after IS change.

This suggested approach cannot be implemented in the other commonly adopted procedures where salt addition is made at the lowest pH value[22,23] because E_{drift} is then not measurable. The current approach offers the advantage to perform the entire titration procedure in the same sample, without performing additional titration at fixed pH vs. salt concentration.[30] As a result, this procedure saves both time and lab work effort while eliminating possible experimental biases.

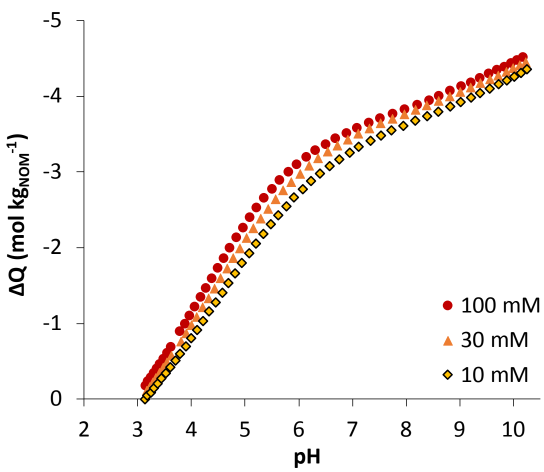

Figure 2: Change in SRFA charge versus pH in comparison to the situation at pH 3 (ΔQ), as measured at 10 mM, 30 mM and 100 mM NaCl.

Fitting proton affinity spectra: absolute curve positioning by Q_0 determination. ΔQ values provide limited information on HS acid-base properties. An absolute positioning of the titration curves is required to fully address HS charge (Q). As described in the experimental section, Q_0 is obtained via fitting the experimental proton affinity spectra ($dQ/d(pH)$) using SPBT-PEST iterative procedure. We recall that the initial guessed estimates of the parameters involved in SPBT model (r_p, M_w, $Q_{max,1}$, $Q_{max,2}$, pKa$_1$, pKa$_2$, m_1, m_2), used to initiate the iterative computational process for reconstruction of proton affinity curves, are listed in Table S1 for all HS materials analyzed in this work.

Theoretical reconstruction of the proton affinity spectra is illustrated in Figure 3a for SRFA. Corresponding fitting provides a full set of newly adjusted SPBT parameters. These adjusted parameters are then subsequently adopted to theoretically compute the charge curves (Q) for each ionic strength tested. These theoretical curves are shifted to more negative charge values (Figure 3b) as compared to measured ones simply because they account for the negative electrical charge that HS material already carries under the starting conditions of the titration measurement (i.e. pH = 3, 10 mM NaCl). Under such initial conditions, ΔQ was set to 0 as a result of the blank subtraction. Accordingly, the value of the absolute charge Q_0 is directly inferred from calculated Q at pH = 3 in 10 mM NaCl.

The Q_0 values (given in mol kg^{-1}) obtained for the different IHSS samples of interest in this work (see the corresponding experimental and reconstructed proton titration curves in Figure S2, section E in SI) were found to be larger for tested fulvic acids and NOM (SRFA -1.00, PPFA -1.75, SRNOM -1.27) than for the humic acids (SRHA -0.69, PPHA -0.62, LHA -0.70, ESHA -0.94), in line with the larger overall charge and acidity of fulvic acids known for IHSS samples.[26] The developed method was applied to the most recently extracted and purified IHSS samples (next section).

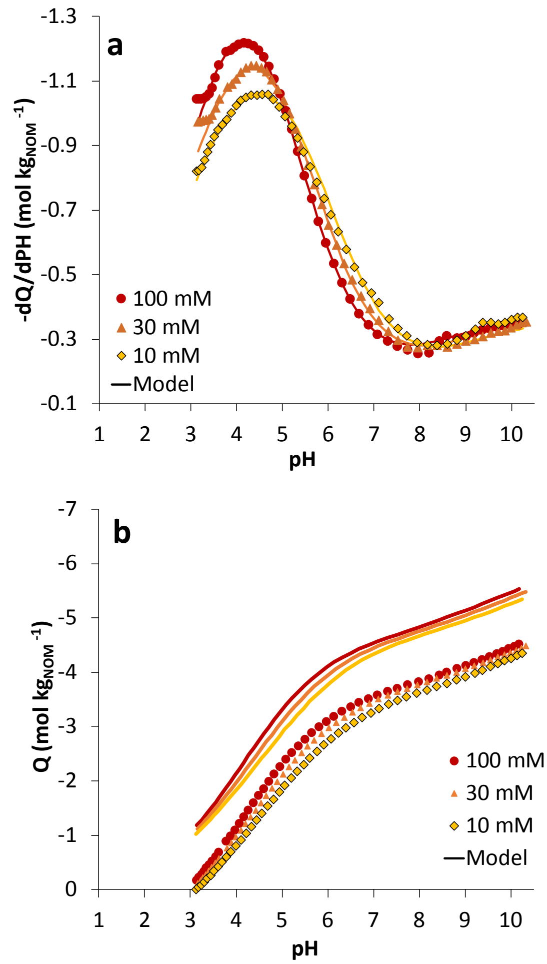

Figure 3: (a) Experimental and modeled proton affinity spectra for SRFA (d*Q*/dpH versus pH) at three IS (10 mM, 30 mM, 100 mM). (b) Experimental Δ*Q* (symbols) and simulated *Q* (lines) (versus pH and salt concentration) by SPBT-PEST for SRFA versus pH at three IS (10 mM, 30 mM, 100 mM). In both panels, experimental data are represented by symbols whereas modeled results are plotted by solid lines with the same color code as that for corresponding experimental data.

IHSS samples, thirty years after. The corrected proton titration curves established for the whole set of here studied HS materials are compared with those obtained for the first IHSS samples analyzed at 0.1 M ionic strength by Ritchie and Perdue[26], recalling that the latter samples were extracted and purified about 30 years ago. When comparing Δ*Q* plotted from both data sets (data acquired by Ritchie and Perdue[26] and data acquired in this study) at pH 3, a difference of less than 5% is obtained (Figure S3, section F in SI). This may suggest that the temporal variability of HS acid-base properties is rather small. A detailed comparison can be carried by recalculating the charge values published by Ritchie and perdue[26] at 0.1 M IS using modified Henderson-Hasselbalch model with optimized parameters (denoted as Q_1', Q_2', Log k_1 , Log k_2, n_1 and n_2 in Ritchie and Perdue[26]) and converting into mol kg^{-1} of NOM from values in meq gC^{-1}. We found that the experimental total HS charge is larger than that measured in this work (Figure S4, section G in SI) due to a larger Q_0 determined by Ritchie and Perdue.[26] This leads to different proportions of functional groups as exemplified for SRFA by the ca. 4 to 1 carboxylic to phenolic ratio reported by Ritchie and Perdue[26] as well as in other studies[25,33] which is higher than the 2 to 1 ratio obtained in the current study. This comparison emphasizes how differences in computation of Q_0 (i.e. absolute positioning of titration curves) leads to possible misevaluation of carboxylic sites density. We stress that HS charge evaluation in Ritchie and Perdue[26] is based on an approach assuming that all carboxyl groups and no phenolic groups are titrated at pH 8 and that one half of the phenolic groups are titrated between pH 8 and pH 10. We argue that our model fits all experimental data without such *a priori* assumption. In addition, a prerequisite for the application of the Henderson-Hasselbalch equation adopted in Ritchie and Perdue[26] (without any electrostatic component included) is that data subjected to fitting using that equation must necessarily refer to a so-called master curve (i.e. all HS charges are completely screened and there is no polyelectrolyte effect at stake). Obviously, any simple look at the data cannot directly and quantitatively inform on the presence/absence of electrostatic effects, and the hypothesis underlying a valid application of the Henderson-Hasselbalch equation (without electrostatic component included) is -to the best of our knowledge- rarely justified. By contrast, our approach combining HS charge evaluation at different IS allows for refined and consistent consideration of HS electrostatics.

SPBT parameters refinement. Using the determined Q_0 values, all ΔQ titration data could be converted into an absolute charge scale (Q). A refinement of the SPBT parameters was then carried out by simultaneous fitting of both Q and dQ/dpH vs. pH curves [18] using as initial guessed parameter values those derived from SPBT-PEST-based fitting of the proton affinity spectra. The refined parameters for the 7 here-examined samples (SRFA, SRHA, SRNOM, PPFA, PPHA, LHA, ESHA) are collected in Table 1. The experimental and SPBT-PEST modeled titration curves are all displayed in Figure 4 for SRFA, and in Figure S2 for the other six IHSS samples. All modeled curves are in remarkable agreement with the measured titration curves.

The fitted r_p values do not significantly differ from the measured ones for most of HS samples, except for PPFA with r_p =1.56 ± 0.34 nm (measured) and 2.75 ± 0.14 nm (fitted value), and PPHA with r_p =3.04 ± 0.25 nm (measured) and 3.67 ± 0.28 nm (fitted). As a possible explanation for these deviations, it can be argued that SSCP used for the determination of r_p

(Section A in SI) is more sensitive towards smaller particles that diffuse faster.[53] Therefore, in a polydisperse system this measurement may be biased by the presence of small particles, possibly leading to an underestimation of the mean particle size of the sample.

All fitted values of M_w fall within the intervals of measured values reported in literature (Table S1). In detail, fitted values of M_w were close to $M_{w,min}$ values given for SRFA, SRNOM, PPFA, LHA and ESHA, whereas those of PPHA lie in the mid-range in the interval 6.4 to 19.2 kg mol^{-1} with a fitted value of 11.10 kg mol^{-1}. For SRHA, M_w = 4.02 kg mol^{-1} compares to $M_{w,max}$ (4.4 kg mol^{-1}).

The retrieved size and molecular weight seem to differ according to the respective origins of the tested samples. The river-extracted samples indeed display - in average - smaller r_p (ranging from 0.8 to 1.8 nm) and M_w (ranging from 1.14 to 4.02 kg mol^{-1}) than the peat and soil ones ($1.71 < r_p < 3.67$ nm; $3.64 < M_w < 11.10$ kg mol^{-1}). Furthermore, some similarities can be drawn between samples of the same nature, as humic particles samples are larger and heavier than fulvic ones.[61] These results are supported by other studies that associate larger and heavier particles to terrestrial refractory molecules originating from plant residues, and smaller and lighter particles associated to more labile particles such as bacterial-sourced organic matter. [62,63] No such cluster is observed regarding the $Q_{max,i}$, pKa$_i$ and m_i parameters (with i = 1 or 2). The acidity constants are distributed from 3.29 to 4.33 and from 9.24 to 11.31 for carboxylic and phenolic sites, respectively. Also, the heterogeneity parameters are in average 0.51 ± 0.068 and 0.28 ± 0.10 for carboxylic and phenolic sites, respectively.

The obtained density of carboxylic sites ranges from to 3.31 to 6.42 mol kg^{-1}, whereas that of the phenolic sites lies in between 1.10 and 4.48 mol kg^{-1}. The carboxylic-to-phenolic site density ratios ranges from 0.8 (for ESHA and PPHA) to 5.8 (for PPFA). Table S2 (section H in SI) compares site densities ratios of carboxylic and phenolic groups in IHSS samples from several studies [26,25,64] with results obtained from this work. Although different data acquisition and treatment methods were used in these various studies, they systematically report $Q_{max,1} > Q_{max,2}$, in contrast to our findings. Most of the models describing titration curves used in the studies with which our carboxylic-to-phenolic ratios are compared,[25,26,64] do not explicitly account for the electrostatic contribution to protons binding. Also, as mentioned in the introduction section, there is no clear explanation as how Q_0 was determined in these studies. For these reasons, we hypothesize that the carboxylic to phenolic ratio found therein might have been misevaluated. Consequently, we argue that inaccuracy in determining Q_0 and in describing the titration curves with unsuitable chemical-electrostatic model may have significant implications for the estimation of parameters pertaining to the intrinsic chemical component of HS charge.

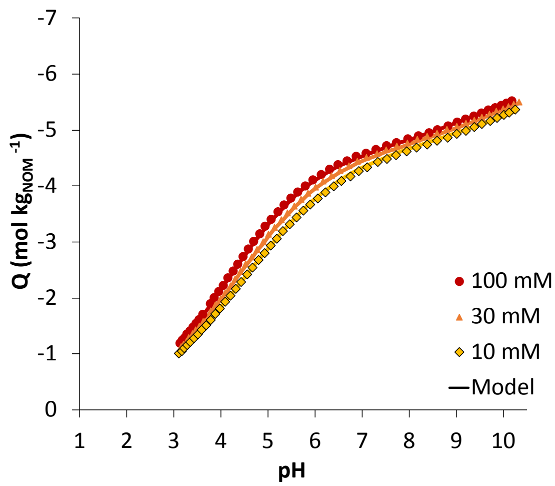

Figure 4: Fully corrected experimental titration curves (symbols) and SPBT modelled titration curves (plain lines) for SRFA at 10 mM, 30 mM and 100 mM of NaCl.

Table 1: Optimized chemical parameters retrieved from SPBT-PEST modelling of titration data and associated proton affinity spectra.

Sample	$Q_{max,1}$ mol kg^{-1}	$Q_{max,2}$ mol kg^{-1}	pKa_1	pKa_2	m_1	m_2	r_p (nm)	M_w kg mol^{-1}
SRFA	-4.35 ± 0.06	-2.40 ± 0.30	3.76 ± 0.01	9.50 ± 0.28	0.57 ± 0.01	0.26 ± 0.03	1.34 ± 0.03	1.51 ± 0.06
SRHA	-3.31 ± 0.15	-3.87 ± 0.98	3.80 ± 0.02	10.04 ± 0.65	0.54 ± 0.02	0.24 ± 0.05	1.80 ± 0.03	4.02 ± 0.01
SRNOM	-4.33 ± 0.05	-3.38 ± 0.27	3.26 ± 0.01	9.73 ± 0.25	0.58 ± 0.01	0.24 ± 0.01	0.89 ± 0.04	1.15 ± 0.09
PPFA	-6.42 ± 0.02	-1.10 ± 0.05	3.66 ± 0.01	9.43 ± 0.09	0.40 ± 0.01	0.46 ± 0.02	2.75 ± 0.14	3.64 ± 1.09
PPHA	-3.40 ± 0.26	-4.26 ± 2.35	4.04 ± 0.02	11.31 ± 1.83	0.52 ± 0.03	0.20 ± 0.06	3.67 ± 0.28	11.10 ± 3.30
LHA	-4.01 ± 0.13	-2.00 ± 0.37	4.33 ± 0.05	9.24 ± 0.21	0.43 ± 0.01	0.41 ± 0.07	3.39 ± 0.37	5.78 ± 5.24
ESHA	-3.74 ± 0.12	-4.48 ± 1.34	3.27 ± 0.02	10.76 ± 1.06	0.51 ± 0.02	0.20 ± 0.02	1.71 ± 0.15	7.69 ± 3.21

Environmental implications

Potentiometric acid-base titration of nanoparticulate HS at different salt concentrations is a method of choice to determine HS charge properties. A proper interpretation of the corresponding data and ensuing evaluation of proton-HS binding is a mandatory pre-requisite for addressing at a mechanistic level the reactivity of HS with respect to e.g. metal ions or mineral surfaces. Correctness in such data interpretation is tied to: (i) adequate positioning of the raw proton titration curves measured at different salt concentrations and their correction for blank titration, and (ii) appropriate deciphering of the intrinsic chemical and non-specific electrostatic contributions to proton binding. The potentiometric acid-base titration protocol developed in this work for characterizing HS charging behavior and the corresponding data analysis methodology we propose overcome most of the so-far unresolved technical limitations and biases that we herein identify. Our theoretical interpretative framework further solves the inherent shortcomings of conventional thermodynamic models largely used for the analysis of proton titration HS data but unfortunately based on an flawed representation of the electrostatics operational for soft nano-HS particles.

Significant discrepancies are evidenced from comparison between proton titration datasets established in this study for a large range of newly analyzed IHSS substances, and those available in literature for similar samples. Outcome thus pinpoints possible flawed experimental setup and/or unclear or even inappropriate data treatment methods adopted in the past. A major point of concern is that these literature data have been extensively used to calibrate empirical and phenomenological models for 'predicting' HS reactivity, putting aside the large limitations of these models in their account of the true potential distribution in the intra- and extra-particulate HS spatial regions. As a result, reactive HS site densities and especially dissociation constants of carboxylic and phenolic HS functional groups reported in literature are likely subjected to some uncertainties. In turn, predictions of HS reactivity towards protons or even metal species as reported on the basis of such biased experimental titration data and analysis thereof should be considered with caution. For the sake of illustration, whereas carboxylic sites are generally considered to be more abundant than phenolic groups, the results detailed in this work add much nuance to this accepted property, depending on the type of considered HS material. When comparing the *relative* HS charge variation (relative to HS charge at pH 3) at 0.1M solution ionic strength, we observe small differences (less than 5%) between acid-base properties of 7 HS samples newly provided by the IHSS and those derived from data collected on equivalent samples extracted 30 years ago. Because these HS samples largely serve as reference to investigate NOM reactivity towards metal ions, a re-evaluation of cations-HS binding data and modeling may be achieved with improved consideration of the electrostatic component of protons binding and with caution to relative and absolute curves positioning, as done in this work.

By analyzing 7 IHSS samples, a notable variability in proton-HS affinity is evaluated. As previously reported, humic or fulvic samples show similarities, especially with respect to their size and molecular weight, which was a major argument for past establishment of generic parameters for popular HS reactivity models. However, HS from aquatic and terrestrial origins define two types of HS and HA/FA grouping with respect to their overall charge behavior. In line with previous criticisms formulated on empirical NICA-Donnan modeling, we recommend to perform potentiometric acid-base titration and we advocate for the derivation of specific interpretation of data collected on samples of interest rather than resort to the use of generic parameters. This work provides reliable tools and fast methodological strategy to achieve these required tasks and to better understand HS reactivity to metal ions or mineral surfaces, as required in the analysis of numerous major environmental issues.

Acknowledgments

This work was supported by the C-FACTOR project funded by ANR (project number ANR-18-CE01-0008; coordinator: R. Marsac). This work was carried out in the Pôle de compétences Physico-Chimie de l'Environnement, LIEC laboratory UMR 7360 CNRS - Université de Lorraine.

References

(1) Berner, R. A. Jacques-Joseph Ébelmen, the Founder of Earth System Science. *Comptes Rendus Geosci.* **2012**, *344* (11–12), 544–548. https://doi.org/10.1016/j.crte.2012.08.001.

(2) Prentice, I. C.; Farquhar, G. D.; Fasham, M. J. R.; Goulden, M. L.; Heimann, M.; Jaramillo, V. J.; Kheshgi, H. S.; LeQuéré, C.; Scholes, R. J.; Wallace, D. W. R. The Carbon Cycle and Atmospheric Carbon Dioxide. In *Climate Change 2001: the Scientific Basis. Contributions of Working Group I to the Third Assessment Report of the Intergovernmental Panel on Climate Change*; Houghton, J. T., Ding, Y., Griggs, D. J., Noguer, M., van der Linden, P. J., Dai, X., Maskell, K., Johnson, C. A., Eds.; Cambridge University Press: Cambridge, UK, 2001; pp 185–237.

(3) Raich, J. W.; Potter, C. S. Global Patterns of Carbon Dioxide Emissions from Soils. *Glob. Biogeochem. Cycles* **1995**, *9* (1), 23–36. https://doi.org/10.1029/94GB02723.

(4) Kinniburgh, D. G.; van Riemsdijk, W. H.; Koopal, L. K.; Borkovec, M.; Benedetti, M. F.; Avena, M. J. Ion Binding to Natural Organic Matter: Competition, Heterogeneity, Stoichiometry and Thermodynamic Consistency. *Colloids Surf. Physicochem. Eng. Asp.* **1999**, *151* (1–2), 147–166. https://doi.org/10.1016/S0927-7757(98)00637-2.

(5) Buffle, J. Complexation Reactions in Aquatic Systems; Analytical Approach. *Acta Hydrochim. Hydrobiol.* **1989**, *17* (2), 230–230. https://doi.org/10.1002/aheh.19890170220.

(6) Schnitzer, M. Effect of Low pH on the Chemical Structure and Reaction of Humic Substances. In *Effects of Acid Precipitation on Terrestrial Ecosystems*; Hutchinson, T. C., Havas, M., Eds.; Springer US: Boston, MA, 1980; pp 203–222. https://doi.org/10.1007/978-1-4613-3033-2_18.

(7) Benedetti, M. F.; Milne, C. J.; Kinniburgh, D. G.; Van Riemsdijk, W. H.; Koopal, L. K. Metal Ion Binding to Humic Substances: Application of the Non-Ideal Competitive Adsorption Model. *Environ. Sci. Technol.* **1995**, *29* (2), 446–457. https://doi.org/10.1021/es00002a022.

(8) Marang, L.; Eidner, S.; Kumke, M. U.; Benedetti, M. F.; Reiller, P. E. Spectroscopic Characterization of the Competitive Binding of Eu(III), Ca(II), and Cu(II) to a Sedimentary Originated Humic Acid. *Chem. Geol.* **2009**, *264* (1–4), 154–161. https://doi.org/10.1016/j.chemgeo.2009.03.003.

(9) Marsac, R.; Catrouillet, C.; Davranche, M.; Bouhnik-Le Coz, M.; Briant, N.; Janot, N.; Otero-Fariña, A.; Groenenberg, J. E.; Pédrot, M.; Dia, A. Modeling Rare Earth Elements Binding to Humic Acids with Model VII. *Chem. Geol.* **2021**, *567*, 120099. https://doi.org/10.1016/j.chemgeo.2021.120099.

(10) Milne, C. J.; Kinniburgh, D. G.; van Riemsdijk, W. H.; Tipping, E. Generic NICA−Donnan Model Parameters for Metal-Ion Binding by Humic Substances. *Environ. Sci. Technol.* **2003**, *37* (5), 958–971. https://doi.org/10.1021/es0258879.

(11) Pinheiro, J. P.; Mota, A. M.; Benedetti, M. F. Effect of Aluminum Competition on Lead and Cadmium Binding to Humic Acids at Variable Ionic Strength. *Environ. Sci. Technol.* **2000**, *34* (24), 5137–5143. https://doi.org/10.1021/es0000899.

(12) Tipping, E.; Rey-Castro, C.; Bryan, S. E.; Hamilton-Taylor, J. Al(III) and Fe(III) Binding by Humic Substances in Freshwaters, and Implications for Trace Metal Speciation. *Geochim. Cosmochim. Acta* **2002**, *66* (18), 3211–3224. https://doi.org/10.1016/S0016-7037(02)00930-4.

(13) Marsac, R.; Banik, N. L.; Lützenkirchen, J.; Catrouillet, C.; Marquardt, C. M.; Johannesson, K. H. Modeling Metal Ion-Humic Substances Complexation in Highly Saline Conditions. *Appl. Geochem.* **2017**, *79*, 52–64. https://doi.org/10.1016/j.apgeochem.2017.02.004.

(14) Thurman, E. M.; Wershaw, R. L.; Malcolm, R. L.; Pinckney, D. J. Molecular Size of Aquatic Humic Substances. *Org. Geochem.* **1982**, *4* (1), 27–35. https://doi.org/10.1016/0146-6380(82)90005-5.

(15) Slaveykova, V. I.; Wilkinson, K. J. Predicting the Bioavailability of Metals and Metal Complexes: Critical Review of the Biotic Ligand Model. *Environ. Chem.* **2005**, *2* (1), 9–24. https://doi.org/10.1071/EN04076.

(16) Van Leeuwen, H. P. Metal Speciation Dynamics and Bioavailability: Inert and Labile Complexes. *Environ. Sci. Technol.* **1999**, *33* (21), 3743–3748. https://doi.org/10.1021/es990362a.

(17) Van Leeuwen, H. P.; Duval, J. F. L.; Paulo Pinheiro, J.; Blust, R.; M. Town, R. Chemodynamics and Bioavailability of Metal Ion Complexes with Nanoparticles in Aqueous Media. *Environ. Sci. Nano* **2017**, *4* (11), 2108–2133. https://doi.org/10.1039/C7EN00625J.

(18) Pinheiro, J. P.; Rotureau, E.; Duval, J. F. L. Addressing the Electrostatic Component of Protons Binding to Aquatic Nanoparticles Beyond the Non-Ideal Competitive Adsorption (NICA)-Donnan Level: Theory and Application to Analysis of Proton Titration Data for Humic Matter. *J. Colloid Interface Sci.* **2021**, *583*, 642–651. https://doi.org/10.1016/j.jcis.2020.09.059.

(19) Town, R. M.; van Leeuwen, H. P.; Duval, J. F. L. Rigorous Physicochemical Framework for Metal Ion Binding by Aqueous Nanoparticulate Humic Substances: Implications for Speciation Modeling by the NICA-Donnan and WHAM Codes. *Environ. Sci. Technol.* **2019**, *53* (15), 8516–8532. https://doi.org/10.1021/acs.est.9b00624.

(20) Tipping, E.; Lofts, S.; Sonke, J. E. Humic Ion-Binding Model VII: A Revised Parameterisation of Cation-Binding by Humic Substances. *Environ. Chem.* **2011**, *8* (3), 225. https://doi.org/10.1071/EN11016.

(21) Koopal, L. K.; Saito, T.; Pinheiro, J. P.; Riemsdijk, W. H. van. Ion Binding to Natural Organic Matter: General Considerations and the NICA–Donnan Model. *Colloids Surf. Physicochem. Eng. Asp.* **2005**, *265* (1–3), 40–54. https://doi.org/10.1016/j.colsurfa.2004.11.050.

(22) Benedetti, M. F.; Van Riemsdijk, W. H.; Koopal, L. K. Humic Substances Considered as a Heterogeneous Donnan Gel Phase. *Environ. Sci. Technol.* **1996**, *30* (6), 1805–1813. https://doi.org/10.1021/es950012y.

(23) Nederlof, M. M.; De Wit, J. C. M.; Van Riemsdijk, W. H.; Koopal, L. K. Determination of Proton Affinity Distributions for Humic Substances. *Environ. Sci. Technol.* **1993**, *27* (5), 846–856. https://doi.org/10.1021/es00042a006.

(24) Ephraim, James.; Alegret, Salvador.; Mathuthu, Andrew.; Bicking, Margaret.; Malcolm, R. L.; Marinsky, J. A. A Unified Physicochemical Description of the Protonation and Metal Ion Complexation Equilibria of Natural Organic Acids (Humic and Fulvic Acids). 2. Influence of Polyelectrolyte Properties and Functional Group Heterogeneity on the Protonation Equilibria of Fulvic Acid. *Environ. Sci. Technol.* **1986**, *20* (4), 354–366. https://doi.org/10.1021/es00146a007.

(25) Milne, C. J.; Kinniburgh, D. G.; Tipping, E. Generic NICA-Donnan Model Parameters for Proton Binding by Humic Substances. *Environ. Sci. Technol.* **2001**, *35* (10), 2049–2059. https://doi.org/10.1021/es000123j.

(26) Ritchie, J. D.; Perdue, E. M. Proton-Binding Study of Standard and Reference Fulvic Acids, Humic Acids, and Natural Organic Matter. *Geochim. Cosmochim. Acta* **2003**, *67* (1), 85–96. https://doi.org/10.1016/S0016-7037(02)01044-X.

(27) Vermeer, A. W. P.; van Riemsdijk, W. H.; Koopal, L. K. Adsorption of Humic Acid to Mineral Particles. 1. Specific and Electrostatic Interactions. *Langmuir* **1998**, *14* (10), 2810–2819. https://doi.org/10.1021/la970624r.

(28) Lenoir, T.; Matynia, A.; Manceau, A. Convergence-Optimized Procedure for Applying the NICA-Donnan Model to Potentiometric Titrations of Humic Substances. *Environ. Sci. Technol.* **2010**, *44* (16), 6221–6227. https://doi.org/10.1021/es1015313.

(29) Brassard, P.; Kramer, J. R.; Collins, P. V. Binding Site Analysis Using Linear Programming. *Environ. Sci. Technol.* **1990**, *24* (2), 195–201. https://doi.org/10.1021/es00072a006.

(30) Tan, W. F.; Koopal, L. K.; Weng, L. P.; van Riemsdijk, W. H.; Norde, W. Humic Acid Protein Complexation. *Geochim. Cosmochim. Acta* **2008**, *72* (8), 2090–2099. https://doi.org/10.1016/j.gca.2008.02.009.

(31) Driver, S. J.; Perdue, E. M. Acidic Functional Groups of Suwannee River Natural Organic Matter, Humic Acids, and Fulvic Acids. In *ACS Symposium Series*; Rosario-Ortiz, F., Ed.; American Chemical Society: Washington, DC, 2014; Vol. 1160, pp 75–86. https://doi.org/10.1021/bk-2014-1160.ch004.

(32) Sasaki, T.; Kobayashi, T.; Takagi, I.; Moriyama, H. Discrete Fragment Model for Complex Formation of Europium(III) with Humic Acid. *J. Nucl. Sci. Technol.* **2008**, *45* (8), 718–724. https://doi.org/10.1080/18811248.2008.9711472.

(33) Tipping, E. Humic Ion-Binding Model VI: An Improved Description of the Interactions of Protons and Metal Ions with Humic Substances. *Aquat. Geochem.* **1998**, *4* (1), 3–47. https://doi.org/10.1023/A:1009627214459.

(34) Chen, W.; Guéguen, C.; Smith, D. S.; Galceran, J.; Puy, J.; Companys, E. Comparing a Fully Optimized ContinUouS (FOCUS) Method with the Analytical Inversion of Non Ideal Competitive Adsorption (NICA) for Determining the Conditional Affinity Spectrum (CAS) of H and Pb Binding to Natural Organic Matter. *Colloids Surf. Physicochem. Eng. Asp.* **2022**, *633*, 127785. https://doi.org/10.1016/j.colsurfa.2021.127785.

(35) Sips, R. On the Structure of a Catalyst Surface. *J. Chem. Phys.* **1948**, *16* (5), 490. https://doi.org/10.1063/1.1746922.

(36) Duval, J. F. L.; Wilkinson, K. J.; van Leeuwen, H. P.; Buffle, J. Humic Substances Are Soft and Permeable: Evidence from Their Electrophoretic Mobilities †. *Environ. Sci. Technol.* **2005**, *39* (17), 6435–6445. https://doi.org/10.1021/es050082x.

(37) Duval, J. F. L.; Ohshima, H. Electrophoresis of Diffuse Soft Particles. *Langmuir* **2006**, *22* (8), 3533–3546. https://doi.org/10.1021/la0528293.

(38) Maurya, S. K.; Gopmandal, P. P.; Ohshima, H.; Duval, J. F. L. Electrophoresis of Composite Soft Particles with Differentiated Core and Shell Permeabilities to Ions and Fluid Flow. *J. Colloid Interface Sci.* **2020**, *558*, 280–290. https://doi.org/10.1016/j.jcis.2019.09.118.

(39) van Leeuwen, H. P.; Buffle, J.; Duval, J. F. L.; Town, R. M. Understanding the Extraordinary Ionic Reactivity of Aqueous Nanoparticles. *Langmuir* **2013**, *29* (33), 10297–10302. https://doi.org/10.1021/la401955x.

(40) Hosse, M.; Wilkinson, K. J. Determination of Electrophoretic Mobilities and Hydrodynamic Radii of Three Humic Substances as a Function of PH and Ionic Strength. *Environ. Sci. Technol.* **2001**, *35* (21), 4301–4306. https://doi.org/10.1021/es010038r.

(41) Petrášek, Z.; Schwille, P. Precise Measurement of Diffusion Coefficients Using Scanning Fluorescence Correlation Spectroscopy. *Biophys. J.* **2008**, *94* (4), 1437–1448. https://doi.org/10.1529/biophysj.107.108811.

(42) Vanýsek, P. *CRC Handbook of Chemistry and Physics*, Boca Raton.; CRC Press, 1992.

(43) Town, R. M.; Duval, J. F. L.; van Leeuwen, H. P. The Intrinsic Stability of Metal Ion Complexes with Nanoparticulate Fulvic Acids. *Environ. Sci. Technol.* **2018**, acs.est.8b02896. https://doi.org/10.1021/acs.est.8b02896.

(44) Rotureau, E.; Pinheiro, J. P.; Duval, J. F. L. On the Evaluation of the Intrinsic Stability of Indium-Nanoparticulate Organic Matter Complexes. *Colloids Surf. Physicochem. Eng. Asp.* **2022**, *645*, 128859. https://doi.org/10.1016/j.colsurfa.2022.128859.

(45) Alberts, J. J.; Takács, M. Total Luminescence Spectra of IHSS Standard and Reference Fulvic Acids, Humic Acids and Natural Organic Matter: Comparison of Aquatic and Terrestrial Source Terms. *Org. Geochem.* **2004**, *35* (3), 243–256. https://doi.org/10.1016/j.orggeochem.2003.11.007.

(46) Mobed, J. J.; Hemmingsen, S. L.; Autry, J. L.; McGown, L. B. Fluorescence Characterization of IHSS Humic Substances: Total Luminescence Spectra with Absorbance Correction. *Environ. Sci. Technol.* **1996**, *30* (10), 3061–3065. https://doi.org/10.1021/es960132l.

(47) Janot, N.; Reiller, P. E.; Korshin, G. V.; Benedetti, M. F. Using Spectrophotometric Titrations To Characterize Humic Acid Reactivity at Environmental Concentrations. *Environ. Sci. Technol.* **2010**, *44* (17), 6782–6788. https://doi.org/10.1021/es1012142.

(48) Cabaniss, S. E. Carboxylic Acid Content of a Fulvic Acid Determined by Potentiometry and Aqueous Fourier Transform Infrared Spectrometry. *Anal. Chim. Acta* **1991**, *255* (1), 23–30. https://doi.org/10.1016/0003-2670(91)85082-4.

(49) Christensen, J. B.; Tipping, E.; Kinniburgh, D. G.; Grøn, C.; Christensen, T. H. Proton Binding by Groundwater Fulvic Acids of Different Age, Origins, and Structure Modeled with the Model V and NICA−Donnan Model. *Environ. Sci. Technol.* **1998**, *32* (21), 3346–3355. https://doi.org/10.1021/es971134o.

(50) Christl, I.; Metzger, A.; Heidmann, I.; Kretzschmar, R. Effect of Humic and Fulvic Acid Concentrations and Ionic Strength on Copper and Lead Binding. *Environ. Sci. Technol.* **2005**, *39* (14), 5319–5326. https://doi.org/10.1021/es050018f.

(51) Perdue, E. M.; Reuter, J. H.; Ghosal, M. The Operational Nature of Acidic Functional Group Analyses and Its Impact on Mathematical Descriptions of Acid-Base Equilibria in Humic Substances. *Geochim. Cosmochim. Acta* **1980**, *44* (11), 1841–1851. https://doi.org/10.1016/0016-7037(80)90233-1.

(52) Sposito, G.; Holtzclaw, K. M. Titration Studies on the Polynuclear, Polyacidic Nature of Fulvic Acid Extracted from Sewage Sludge-Soil Mixtures. *Soil Sci. Soc. Am. J.* **1977**, *41* (2), 330–336. https://doi.org/10.2136/sssaj1977.03615995004100020031x.

(53) Pinheiro, J. P.; Domingos, R.; Lopez, R.; Brayner, R.; Fiévet, F.; Wilkinson, K. Determination of Diffusion Coefficients of Nanoparticles and Humic Substances Using Scanning Stripping Chronopotentiometry (SSCP). *Colloids Surf. Physicochem. Eng. Asp.* **2007**, *295* (1–3), 200–208. https://doi.org/10.1016/j.colsurfa.2006.08.054.

(54) Baes, C. F.; Mesmer, R. S. The Hydrolysis of Cations. *Berichte Bunsenges. Für Phys. Chem.* **1977**, *81* (2), 245–246. https://doi.org/10.1002/bbpc.19770810252.

(55) Neihof, R. A.; Loeb, G. I. The Surface Charge of Particulate Matter in Seawater. *Limnol. Oceanogr.* **1972**, *17* (1), 7–16. https://doi.org/10.4319/lo.1972.17.1.0007.

(56) Neihof, R. Dissolved Organic Matter in Seawater and the Electric Charge of Immersed Surfaces'. *J. Mar. Res.* **1974**, *32*, 5–12.

(57) Hunter, K. a. Microelectrophoretic Properties of Natural Surface-Active Organic Matter in Coastal Seawater. *Limnol. Oceanogr.* **1980**, *25* (5), 807–822. https://doi.org/10.4319/lo.1980.25.5.0807.

(58) Gerritsen, J.; Bradley, S. W. Electrophoretic Mobility of Natural Particles and Cultured Organisms in Freshwaters1. *Limnol. Oceanogr.* **1987**, *32* (5), 1049–1058. https://doi.org/10.4319/lo.1987.32.5.1049.

(59) Beckett, R.; Le, N. P. The Role or Organic Matter and Ionic Composition in Determining the Surface Charge of Suspended Particles in Natural Waters. *Colloids Surf.* **1990**, *44*, 35–49. https://doi.org/10.1016/0166-6622(90)80185-7.

(60) Ramos, A.; López, S.; López, R.; Fiol, S.; Arce, F.; Antelo, J. M. Effect of the Ionic Strength on the Acid-Base Titration Curves of a Soil Fulvic Acid. *Analusis* **1999**, *27* (5), 414–417. https://doi.org/10.1051/analusis:1999270414.

(61) Weng; Van Riemsdijk, W. H.; Koopal, L. K.; Hiemstra, T. Adsorption of Humic Substances on Goethite: Comparison between Humic Acids and Fulvic Acids. *Environ. Sci. Technol.* **2006**, *40* (24), 7494–7500. https://doi.org/10.1021/es060777d.

(62) Guggenberger, G.; Zech, W.; Haumaier, L.; Christensen, B. T. Land-Use Effects on the Composition of Organic Matter in Particle-Size Separates of Soils: II. CPMAS and Solution 13C NMR Analysis. *Eur. J. Soil Sci.* **1995**, *46* (1), 147–158. https://doi.org/10.1111/j.1365-2389.1995.tb01821.x.

(63) Machado, W.; Franchini, J. C.; de Fátima Guimarães, M.; Filho, J. T. Spectroscopic Characterization of Humic and Fulvic Acids in Soil Aggregates, Brazil. *Heliyon* **2020**, *6* (6), e04078. https://doi.org/10.1016/j.heliyon.2020.e04078.

(64) Fernandes, A. N.; Giacomelli, C.; Giovanela, M.; Vaz, D. O.; Szpoganicz, B.; Sierra, M. M. D. Potentiometric Acidity Determination in Humic Substances Influenced by Different Analytical Procedures. *J. Braz. Chem. Soc.* **2009**, *20* (9), 1715–1723. https://doi.org/10.1590/S0103-50532009000900021.